Carbohydrate Polymers 118 (2015) 119–125

Contents lists available at ScienceDirect

Carbohydrate Polymers

journal homepage: www.elsevier.com/locate/carbpol

Structure and properties of moisture-resistant konjac glucomannan films coated with shellac/stearic acid coating

Xueqin Wei[a,b], Jie Pang[b,**], Changfeng Zhang[a,*], Chengcheng Yu[b], Han Chen[b], Bingqing Xie[b]

[a] Shandong Key Laboratory of Storage and Transportation Technology of Agricultural Products, Jinan 250103, China
[b] College of Food Science, Fujian Agriculture and Forestry University, Fuzhou 350002, China

ARTICLE INFO

Article history:
Received 20 May 2014
Received in revised form 26 October 2014
Accepted 10 November 2014
Available online 15 November 2014

Keywords:
Deacetylated konjac glucomannan
Shellca
The coated film
Water vapor permeability
Moisture-resistant properties

ABSTRACT

A series of moisture-resistant konjac glucomannan films were prepared by coating shellac/stearic acid emulsion on deacetylated konjac glucomannan films (dKGM). The effect of stearic acid content on structure and properties of the coated films were investigated by field emission scanning electron microscopy (FE SEM), Fourier transform infrared spectroscopy (FT-IR), ultraviolet spectroscopy (UV), water vapor permeability (WVP), water uptake, water contact angle, and tensile testing. The results revealed that shellac in the coating adhered intimately to the surface of dKGM film, and provided a substrate for the dispersion of stearic acid which played an important role in enhancement of the moisture barrier properties and mechanical properties of the coated films. The WVP of the coated films decreased from 2.63×10^{-11} to 0.37×10^{-11} g/(m s Pa) and the water contact angle increased from 68° to 101.2° when stearic acid content increased from 0 wt% to 40 wt%, showing the potential applications in food preservation.

1. Introduction

It is well known that the natural polymers are of high safety and environmentally friendly. KGM, a high-molecular weight heteropolysaccharide, is composed of β-(1→4) linked D-glucose and D-mannose in the molar ratio of 1:1.6 with a low degree of acetyl groups at the side chain C-6 position (Li, Ji, Xia, & Li, 2012; Maeda, Shimahara, & Sugiyama, 1980). With good film-forming properties and health-protective functions, KGM shows promise in packaging and coating of food (Jia, Fang, & Yao, 2009). However, the applications of KGM films are limited by its hydrophilic and sensitive to moisture, due to a lot of hydroxyl groups in the repeating units of KGM (Xu, Luo, Lin, Zhuo, & Liang, 2009). In our previous work, based on the study of KGM structure (Jian, Zeng, Xiong, & Pang, 2011; Jian, Wang, Yao, & Pang, 2010), the KGM/curdlan blend films, with the water vapor permeability (WVP) value of 19.53×10^{-11} g/(m s Pa), have been prepared (Wu et al., 2012), showing better moisture-resistant properties than pure curdlan [21.50×10^{-11} g/(m s Pa)] but far from LDPE [0.19×10^{-11} g/(m s Pa)] (Phan The, Debeaufort, Luu, & Voilley, 2008). These results motivate us to carry out further research about the moisture-resistant films based on KGM, using an alternative method.

One way to achieve a moisture-resistant film with barrier against WVP is to coat or add some extra hydrophobic components to the film substrate, and then produce the coated film (Cao, Deng, & Zhang, 2006; Lu & Zhang, 2002; Lu, Zhang, & Xiao, 2004) or bilayer film (Anker, Berntsen, Hermansson, & Stading, 2002; Debeaufort, Quezada-Gallo, Delporte, & Voilley, 2000). In term of the coated films, the regenerated cellulose films coated with interpenetrating polymer networks (IPN) coating exhibit good water resistivity, unfortunately, the natural polymers in IPN coating are less than 30 wt% (Cao et al., 2006), failing to thoroughly utilize renewable resource. In term of the bilayer films, casting lipid onto the protein or polysaccharide films (Anker et al., 2002), the greasy surface, waxy taste and potential rancidity problem of lipids curb their use in food applications (Phan The et al., 2008), despite their WVP have significantly decreased. Hence in this work, one of the major tasks is trying to select other natural hydrophobic polymers as coating materials and coat them on KGM film.

Shellac, obtained by refining the secreton of *Kerria lacca*, is one of the few natural polymer allowed for coating purposes in food, owing to excellent film-forming, high gloss, and poor permeability to gases, acid and water vapor (Byun, Ward, &

* Corresponding author at: Shandong Institute of Commerce and Technology, 4516 Travel Road, Caishi, Licheng District, Jinan 250103, China.
Tel.: +86 531 86330135; fax: +86 531 86330125.
** Corresponding author. Tel.: +86 591 83705076; fax: +86 591 83705076.
E-mail addresses: pang3721941@163.com (J. Pang), zcf202@163.com (C. Zhang).

http://dx.doi.org/10.1016/j.carbpol.2014.11.009
0144-8617/

Whiteside, 2012; Farag & Leopold, 2009; Soradech, Nunthanid, Limmatvapirat, & Luangtana-Anan, 2012). It has also been used for the moisture protection of drugs in the pharmaceutical industry and found to decrease the WVP of edible films (Limmatvapirat et al., 2004; Luangtana-Anan, Nunthanid, & Limmatvapirat, 2010; Soradech, Limatvapirat, & Luangtana-Anan, 2013; Wang, Chen, & He, 2008). Shellac is comprised of polyesters and an ester with polyhydroxypolybasic acids, and insoluble in water but soluble in alcohol and alkaline solution (Limmatvapirat, Limmatvapirat, Puttipipatkhachorn, Nuntanid, & Luangtana-Anan, 2007; Luangtana-Anan, Limmatvapirat, Nunthanid, Wanawongthai, Chalongsuk, & Puttipipatkhachorn, 2007). It is well known that stearic acid, as a component of wax used by nature to create superhydrophobic lotus leaves, has been used in the field of moisture barrier due to its low surface energy (Wu, Pan, & Li, 2010). Moreover, with low cost, low toxicity, and biocompatibility, stearic acid could embed into regenerated cellulose film to form a micro–nano binary structure, resulting in the improvements of hydrophobicity (He, Xu, & Zhang, 2013). However, shellac/stearic acid composite coating has seldom been reported (Phan The et al., 2008; Soradech et al., 2013; Wang et al., 2008).

In this paper, in view of seldom reports on the preparation of the coated films based on KGM, we attempt to prepare a series of moisture-resistant deacetylated konjac glucomannan films (dKGM) coated with shellac/stearic acid, in which stearic acid content ranges from 5 up to 60 wt%. The effect of stearic acid content in the coating layer on interfacial and surface structure, moisture barrier properties, and mechanical properties of the resulting coated films were investigated in detail.

2. Materials and methods

2.1. Materials

Purified konjac glucomannan ($M_w = 3.4 \times 10^5$ g/mol) was purchased from San Ai Konjac Food Co., Ltd. (Sichuan, China). Shellac (food grade) was provided by Kunming Xilaike Bio-technology Co., Ltd. (Kunming, China), which was used without further purification. The stearic acid, Na_2CO_3, NaBr and 98% ethanol purchased from Sinopharm Group Chemical Reagent Co., Ltd. (China) were of analytical grade. Polyethylene glycol 400 (PEG 400) was chemical pure with purity ≥99.7%. Polyethylene film (PE, Top Group Co., Ltd, China) and qualitative filter papers (Hangzhou Tezhongzhiye Co., Ltd, China) were bought and used directly.

2.2. Preparation of the coated films

Deacetylated konjac glucomannan films (dKGM) were obtained after solubilization of 1 g of KGM flour in 100 g of deionized water at room temperature for 2.5 h under a 300 rpm stirring. Subsequently, 0.3 g of Na_2CO_3 was added, keeping stirring for 15 min. The film-forming solution was kept for 30 min under the same conditions without stirring prior to be spread onto polystyrene Petri dishes (PS, 150 mm × 25 mm) to provide a sheet with the thickness of about 5 mm and evaporated in an oven at 55 °C for 5 h to obtain dry films with the thickness of about 30 μm. Then, the films were washed exhaustively with distilled water to remove the residual Na_2CO_3 and evaporated again in an oven at 45 °C for 2 h.

The shellac/stearic acid coating was prepared by dissolving 12 g of shellac particles together with desired content of stearic acid, such as 0 wt%, 5 wt%, 20 wt%, 40 wt% and 60 wt%, in 100 g ethanol under a 300 rpm stirring for 60 min at room temperature. Then, 1.2 g of PEG 400 were added it under a stirring speed at about 5000 rpm (PT 3100 D, KINEMATICA, Switzerland) for 15 min. The resulting mixture solution, namely coating, which prepared from different stearic acid content (0–60 wt%) were denoted SSA0, SSA5, SSA20, SSA40, and SSA60, respectively. The coating was then coated on the both sides of dKGM by brush, and cured at 75 °C for 15 min. The coated films were referred to as dKGM-SSA0, dKGM-SSA5, dKGMSSA20, dKGM-SSA40, dKGM-SSA60, respectively. Before various characterizations, the resulting films were kept in a conditioning desiccator over saturated NaBr solution which fixed 57% RH at room temperature for more than one week to ensure the equilibrium of the water in the films.

2.3. Scanning electron microscopy

Film samples were observed by field emission scanning electron microscopy (FE SEM, Nova NanoSEM230, FEI, America). The films were frozen in liquid nitrogen, immediately snapped, and then dried for the FE SEM observation. The surface of the films was sputtered with platinum for 2.5 min and then observed with 5 kV accelerating voltage.

2.4. Fourier transform infrared spectroscopy

Fourier transform infrared spectroscopy (FT-IR) was carried out with a FT-IR spectrometer (VERTEX 70, Bruker, Germany) in the wavelength range from 4000 to 400 cm^{-1}. The powdered and dried samples were obtained, and the test specimens were prepared by the KBr disk method.

2.5. Ultraviolet spectroscopy

Ultraviolet spectroscopy of films, with thickness of about 38 μm, were carried out with a ultraviolet–visible spectrophotometer (Lambda 800 UV/VIS, Perkin Elmer, America) in the wavelength range from 200 to 800 nm.

2.6. Water vapor permeability determination

Water vapor permeability (WVP) at a relative humidity differential was measured using China National Standard GB 1037-88 (1989) modified by inversing its RH differential, homologous to the ASTM E96-80 (1980). All films used were fixed between two Teflon rings on the top of the glass cell containing distilled water of which the relative humidity is 99% at 25 °C. Test cell was introduced into a climate-controlled chamber (GSP-9160MBE, Shanghai Boxunshiye Co., Ltd., China) regulated at 57% RH and 23 °C; 11% RH and 23 °C or 57% RH and 38 °C. Thus, three relative humidity and temperature differentials (gradients) were used: 57–99% and 23 °C; 11–99% and 23 °C; 57–99% and 38 °C, which mimic a product exposed to different ambient.

Test cell was periodically weighted up to a constant weight variation rate. WVP [g/(m s Pa)] was calculated according to the following equation:

$$\mathrm{WVP} = \frac{\Delta m \times d}{A \times t \times \Delta p}$$

where Δm (g) is the amount of water vapor movement across the film (weight loss); d (mm) is the film thickness; A (mm^2) is the area of the exposed film; Δp (Pa) is the actual difference in partial water vapor pressure between the two sides of the film specimen; t (s) is the time during which a stable weight gain occurred. At least three replicates of each film type were tested for WVP.

2.7. Water uptake measurement

The water uptake of the films was measured according to the procedure described by He, Xu, and Zhang (2013). The films used

were preconditioned at 38 °C for more than two weeks and weighed (W_0). After immersing in distilled water for an expected time, the films were blotted with filter paper to remove the excess water carefully on the surface and weighed (W_t). The water uptake ratio was calculated according to the following equation:

$$\mathrm{WU}(\%) = \frac{M_t - M_0}{M_0} \times 100$$

2.8. Water contact angle testing

Water contact angle was measured and calculated in dynamic mode on a Data Physics Instrument (OCA20). One drop of water (2 μL) was put on the surface of the films with an automatic piston syringe and photographed at time 30 s.

2.9. Practical application: storage of wheat flour in the coated films

Wheat flour was used to test the practical moisture resistance of the coated film dKGM-SSA40 and PE film. As package material, the dKGM-SSA40 and PE films were used to seal the dried vessels (W_0). Then, the vessel which contained wheat flour was weighed (W_1) and introduced into climate-controlled chamber regulated at 34 °C and 99% RH for several period and weighed (W_2) according to ISO 712-1998. The water content ratio of wheat flour was calculated according to the following equation:

$$\mathrm{WC}(\%) = \frac{W_1 - W_2}{W_1 - W_0} \times 100$$

2.10. Mechanical properties

The mechanical properties of the films were measured by a texture analyzer (EZ-TEST, Shimadzu, Japan) according to ISO 527-3-1995 (E) at a speed of 5 mm/min. The specimens (10 mm width) used were 70 mm long. Before characterizations, the resulting films were also kept in a conditioning desiccator over saturated NaBr solution which fixed 57% RH at room temperature for more than one week. And all measurements were made under the same conditions (about 67% RH at 25 °C controlled by air-condition) owing to strength data are related to the environmental temperature and humidity.

3. Results and discussion

3.1. Structure

Fig. 1 shows FT-IR spectra of the SSA0, SSA5, SSA20 and SSA40 coating. The molecule structure of shellac was reported as a polyesters consisting of a number of acidic and hydroxyl side chains (Wang et al., 2008). The broad bands at around 3434 cm^{-1} were attributed to the —OH vibrations from acidic and hydroxyl side chains. The two peaks at around 2930 cm^{-1} and 2861 cm^{-1} were ascribed to the C—H stretching vibrations of $—CH_3$ and $—CH_2$ groups, respectively, while the bending C—H vibrations of $—CH_3$ and $—CH_2$ groups could be found at around 1372 cm^{-1} and 1415 cm^{-1}, respectively. The strong bands at 1729 cm^{-1} and 1640 cm^{-1} were characteristics of C=O groups from acid and ester structures, respectively. For the coating SSA5 and SSA20, the addition of stearic acid to shellac caused an decrease in coating absorption intensity, indicating that shellac and stearic acid had miscibility (Zhang, Xue, Mo, & Jin, 2006, chap. 3). While for SSA40, the location, band width and shape of the absorption band tended to be similar to that of shellac, implying that there are almost immiscibility between shellac and stearic acid in ethanol.

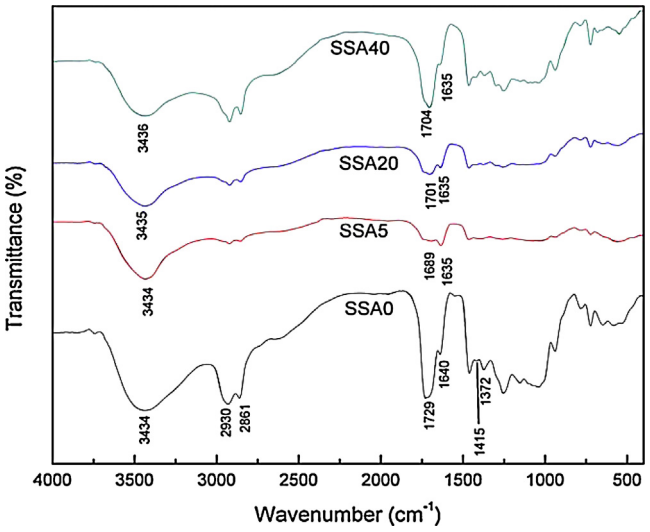

Fig. 1. FT-IR spectra of coating for SSA0, SSA5, SSA20, SSA40.

Fig. 2 shows the FE SEM images of the coated films surface and their coating layer cross-section. The dKGM-SSA0 surface was smooth (Fig. 2a). The surface of the dKGM-SSA5 appeared microscale wrinkle, leading to a slightly rough surface (Fig. 2b). With 20 wt% stearic acid addition, the roughness of the coated film surface became more obvious, exhibiting pitting (Fig. 2c). However, for dKGM-SSA40 and dKGM-SSA60, their surface appeared some extra black spots (Fig. 2d and e). Apparently, it was aggregated stearic acid that made black spots observed.

The micrograph of monolayer SSA0 coating displayed in Fig. 2f. After mixed with 5 wt% stearic acid, the cross section of the coating layer appeared a lot of uniform microgaps (Figs. 2g). The gaps tended to be larger when the content of stearic acid reached 20 wt% (Figs. 2h). It suggested that shellac and 5 wt% or 20 wt% stearic acid in the coating layer mixed uniformly. This can be explained by the fact that shellac and stearic acid were soluble in ethanol but with different solubilities. The solubility of shellac and stearic acid decreased in the process of solvent evaporation (Xie et al., 2004), leading to phase separation, that is, microgaps. On the other hand, shellac acted as continuous phase was a substrate for stearic acid. To minimize the surface energy in the process of solvent evaporation, stearic acid had to aggregate, resulting in gaps for SSA5 and SSA20. Moreover, the evaporation of stearic acid at a very low pressure also cannot be ruled out, because vacuum reached in sputtering process is 1×10^{-3} Pa. For SSA40 and SSA60 (Figs. 2i and j), it was found that the cross section of them exhibited concave structure which confirmed phase separating with heterogeneous structure, suggesting that shellac and 40 wt% or 60 wt% stearic acid could not mix sufficiently. The results were consistent with the conclusions from the FTIR results.

Fig. 3 shows the FE SEM image of the cross section of the coated film. The gray region of about 10 μm thickness on the top is the SSA20 coating layer, and the light region is dKGM substrate. The interface between coating and dKGM appeared to be an intimate adhesion. However, without observing the clear boundary region between the coating layer and dKGM, the coating did not penetrate deeply into the dKGM substrate, indicating that the interaction at the interface belonged to physical interaction. The result conformed with the report in the literature for efficient bonding mechanisms of immiscible polymers (Jannerfeldt, Boogh, & Månson, 2000). Furthermore, the FT-IR spectra of the dKGM and coated films (Fig. A.1 in Appendix A) also indicated that only physical interaction existed between coating layer and dKGM (Cao et al., 2006; Lu & Zhang, 2002; Lu et al., 2004).

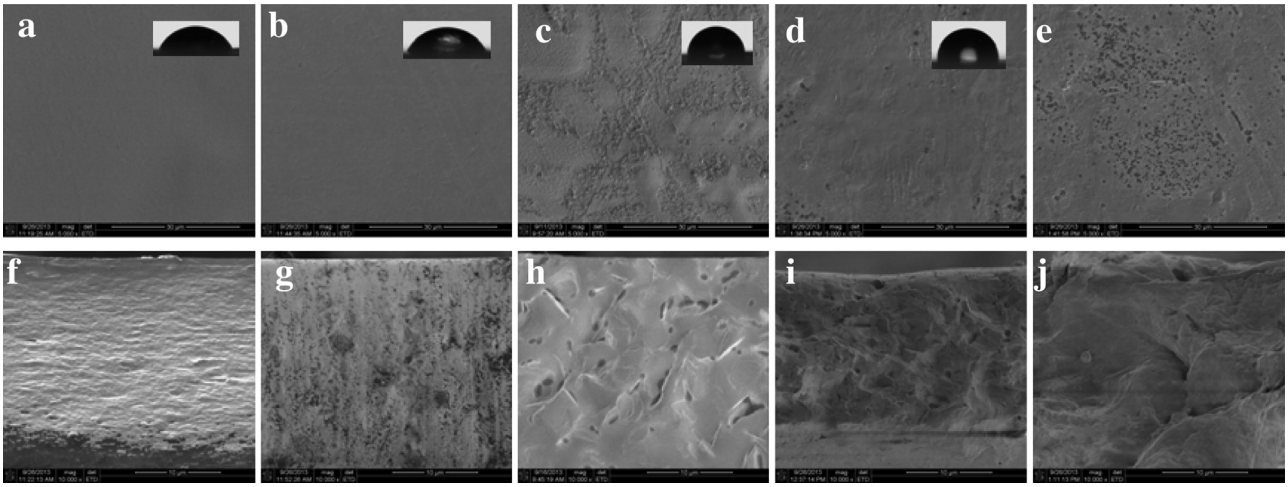

Fig. 2. FE SEM images of surface (top) of the coated films for dKGM-SSA0 (a), dKGM-SSA5 (b), dKGM-SSA20 (c), dKGM-SSA40 (d), dKGM-SSA60 (e) and the cross section (bottom) of the coating for SSA0 (f), SSA5 (g), SSA20 (h), SSA40 (i), SSA60 (j). Insets show the photographs of the water contact angle on each surface after 30 s: dKGM-SSA0 ($68.0 \pm 0.15^{\circ}$), dKGM-SSA5 ($72.1 \pm 2.6^{\circ}$), dKGM-SSA20 ($92.0 \pm 2.2^{\circ}$) and dKGM-SSA40 ($101.2 \pm 1.6^{\circ}$). Scale bars of (a)–(e): 30 μm; scale bars of (f)–(j): 10 μm.

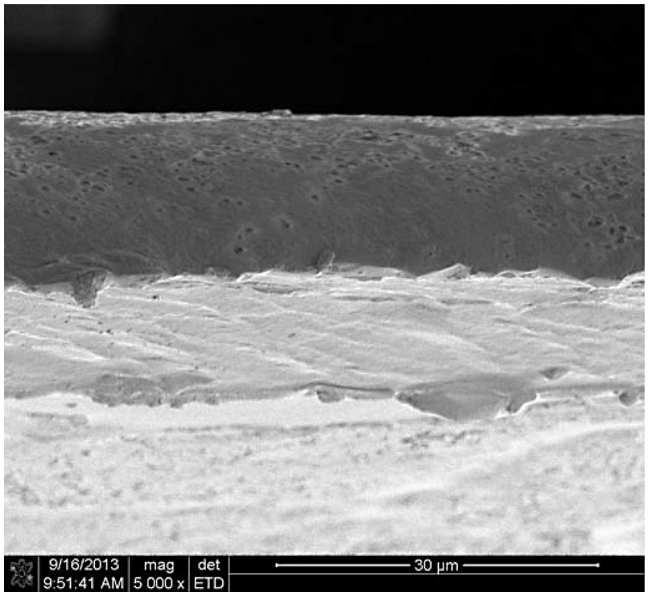

Fig. 3. FE SEM images of the cross section of dKGM-SSA20. Scale bars: 30 μm.

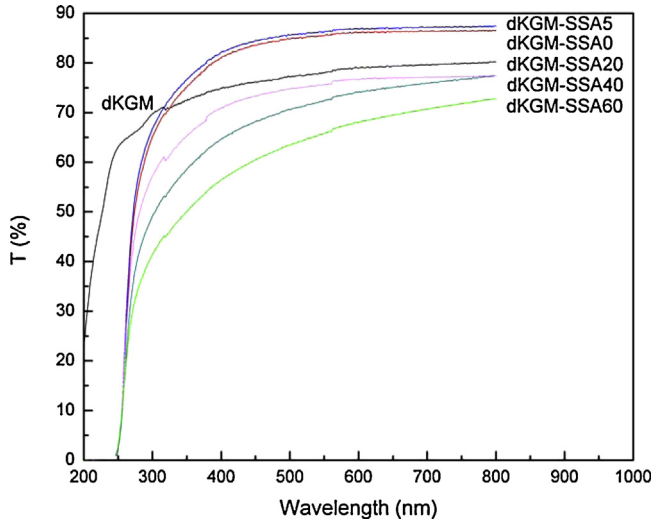

Fig. 4. The optical transmittance (*T*/%) curves of the dKGM and coated films.

The optical transmittance (*T*) curves of the dKGM and coated films are shown in Fig. 4. The transparency of the films is an auxiliary criterion to judge the miscibility of the composite materials (Cao et al., 2006). The interface between two materials will cause losses in optical transmittance, due to the quantity of light that is normally scattered and reflected at the interface of the different solid materials (Lu et al., 2004). Interestingly, with an increase of stearic acid content up to 5 wt%, the *T* values of the coated films were much higher than that of dKGM, and increased nearly to 90%, but then decreased gradually. Enhancement of *T* values of the coated films reflected that the adhesion between the coating layer and dKGM was intimate, and the mixture between shellac and stearic acid in the coating layer was uniformly, which can be explained by the effect of gaps uniformly dispersed throughout the coating layer. Apparently, the *T* value of dKGM-SSA60 film was much lower than that of dKGM-SSA5, which may be attributed to the phase-separated structure in the coating layer. This result was in a good agreement with the conclusions from the FTIR results and FE SEM micrograph. In addition, all the coated films showed obvious ultraviolet absorption capacity at 200–300 nm, indicating the potential application in food packaging.

3.2. Moisture barrier properties

3.2.1. Water vapor permeability

Table 1 shows the WVP of the dKGM, the coated films and PE films which were used as reference for comparison of moisture barrier efficiency. The RH and temperature gradients chosen for this measurement were 57–99% and 23 °C; 11–99% and 23 °C; 57–99% and 38 °C. Tested at 23 °C, the WVP values of the coated films notably decreased with an increase of the stearic acid concentration in the coating layer, reaching the values of 0.60×10^{-11} g/(m s Pa) (at 57–99% differential); 0.79×10^{-11} g/(m s Pa) (at 11–99% differential), respectively, for dKGM-SSA20, which had no significantly difference with dKGM-SSA40 and dKGM-SSA60. This could be explained that the coating layer with higher stearic acid concentration had much better moisture resistance, owing to the hydrophobicity of stearic acid. In addition, the WVP values also decreased with an increase of the stearic acid concentration in the coating layer at 38 °C, but were obviously higher than that of 23 °C. This may be attributed to the thermally unstable of shellac whose softening temperature was at 53.9 °C

Table 1
Water vapor permeability at 23 °C (ΔRH:57–99%; ΔRH: 10–99%) and 38 °C (ΔRH:57–99%) of the dKGM and coated films, compared to PE film.

Samples	Thickness (μm)	Water vapor permeability [10^{-11} g/(m s Pa)]		
		ΔRH:57–99%, 23 °C	ΔRH:11–99%, 23 °C	ΔRH:57–99%, 38 °C
dKGM	38.40 ± 1.40	13.55 ± 1.20	22.48 ± 2.32	33.55 ± 1.88
dKGM-SSA0	36.83 ± 2.84	2.63 ± 0.25 a	4.57 ± 0.38 a	10.95 ± 0.92 a
dKGM-SSA5	37.47 ± 0.83	1.20 ± 0.27 b	2.70 ± 0.19 b	4.47 ± 0.72 b
dKGM-SSA20	37.73 ± 2.53	0.60 ± 0.07 c	0.79 ± 0.19 c	2.30 ± 0.45 c
dKGM-SSA40	38.40 ± 2.42	0.37 ± 0.04 c	n.d.	1.31 ± 0.32 c
dKGM-SSA60	38.60 ± 0.53	0.32 ± 0.10 c	0.58 ± 0.23 c	2.22 ± 0.43 c
PE	12.00	0.08 ± 0.01	0.14 ± 0.03	0.24 ± 0.03

n.d.: not determined. Columns with different letters are significantly different from each other according to Duncan's Multiple Range Test ($P < 0.05$).

(Luangtana-Anan et al., 2007). Although the moisture barrier efficiency of the coated films were still lower than that of PE films [0.14×10^{-11} g/(m s Pa), 11–99% RH at 23 °C] which close to others measurement [0.19×10^{-11} g/(m s Pa), 22–84% RH at 25 °C] (Phan The et al., 2008), the high WVP of dKGM films were remarkably reduced by coating shellac/stearic. With thickness of about 38 μm, the coated films in present work were comparable to the bilayer membranes obtained by depositing a layer of shellac (with thickness of 27.67 μm) onto the surfaces of dried preformed agar- (37.38 μm) or cassava starch-based layers (47.77 μm) (Phan The et al., 2008). Therefore, this work provided a convenient way to prepare thin moisture-resistant films.

3.2.2. Water uptake

To further investigate the water-resistance of the coated films compared with dKGM, the films were soaked in water and the dynamic water uptake plot was measured. The water uptake of the coated film and dKGM immersed in distilled water is shown in Fig. 5. For dKGM, the saturated water uptake ratio reached nearly 200%. As was predicted, the coating layer could reduce the water uptake ratio because of the moisture-resistant buffering effect of the shellac and stearic acid. Moreover, this effect became more significant with an increase of the stearic acid concentration, and the saturated water uptake ratio for dKGM-SSA20 was about 135%. Therefore, the water-resistance ability was improved as a result of the presence of the coating layer.

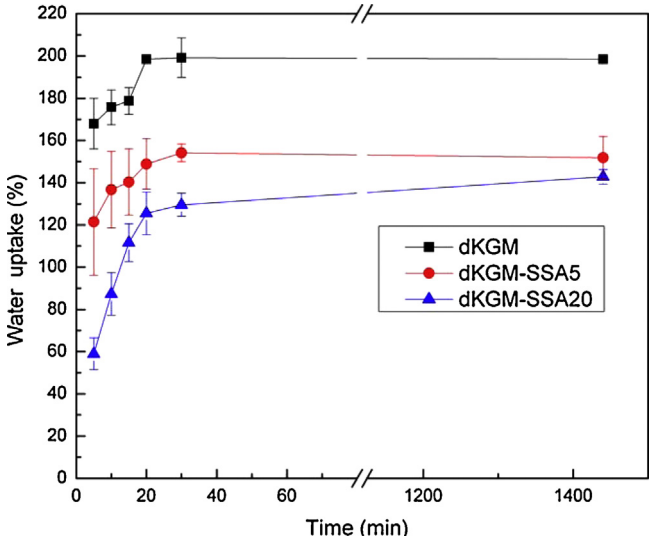

Fig. 5. Water uptake of the dKGM and coated films.

3.2.3. Surface hydrophobicity

Photographs of water drop deposited on the surface of the dKGM and coated films are shown in Fig. 2. It illustrated that the water had a low affinity for the surface of the coated films, which had a relatively high hydrophobicity. The contact angle of dKGM-SSA40 reached a maximum value of 101.2°, which higher than that of dKGM (92.4°). This result further verified that the coated films had better water resistivity than dKGM. It is noted that the contact angles of the coated films increased with an increase of the stearic acid concentration in the coating layer, resulting from higher density of stearic acid in the coating layer. To further demonstrated the contribution of shellac/stearic acid coating to the improvement of the hydrophobicity, a filter paper was coated with shellac/stearic acid also photographed (Fig. A.2 in Appendix A). Therefore, the

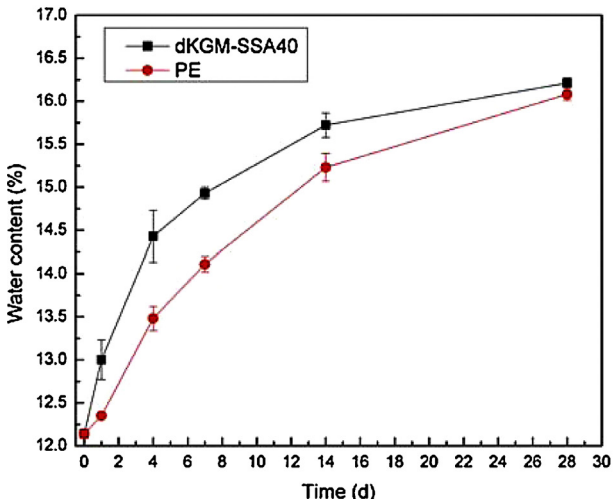

Fig. 6. The time dependence of the water content of wheat flour stored in vessels sealed with the coated films and PE films at 34 °C and 99% RH (left) and photographs of wheat flour stored in vessels sealed with dKGM-SSA40 (a–b) and PE films (c–d) for 0 (a and c) and 28 d (b and d) at 34 °C and 99% RH, respectively (right).

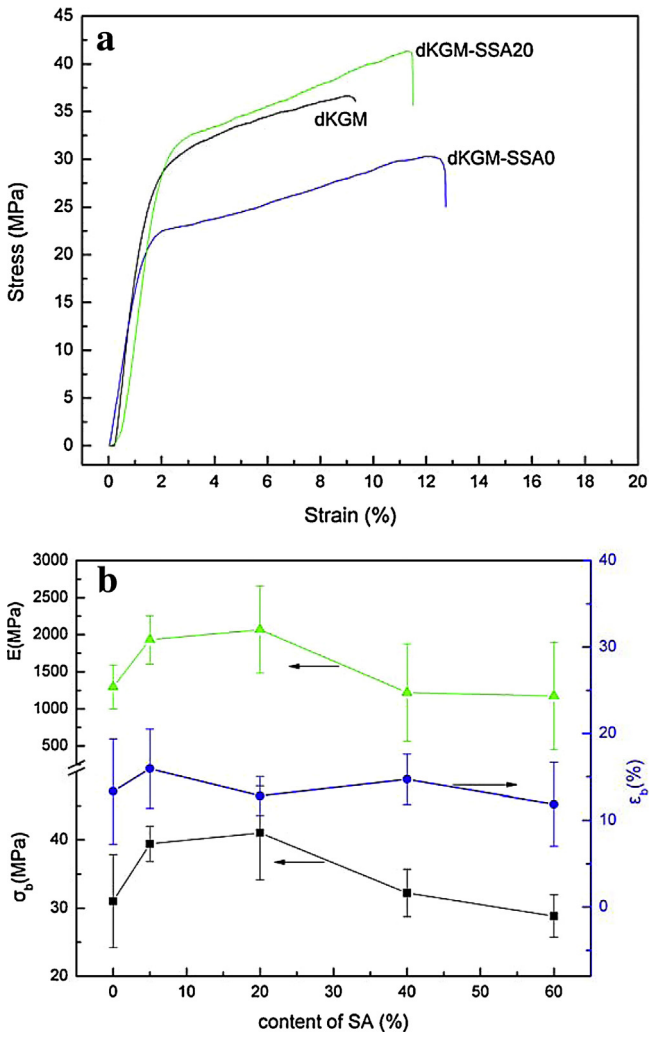

Fig. 7. Stress–strain curves (a) and effect of SA content on tensile strength (σ_b), elongation at break (ε_b) and Young's modulus (E) of the coated films (b).

coating layer consisted of shellac and stearic acid significantly improved the hydrophobicity of the coated films.

3.2.4. *Practical application: storage of wheat flour in the coated films*

Fig. 6 shows the time dependence of the water content (Fig. 6, left) and the photographs (Fig. 6, right) of wheat flour stored in vessels sealed with the coated films and PE films during the stored time. From the curves, water content of wheat flour increased over time and reached almost the same maximum value of 16% at 28 d both for the coated films and PE films, which implied that the moisture barrier efficiency of the coated film was comparable to that of PE. There were no moldy wheat flour observed during 28 d (Fig. 6, right). Therefore, the coated films had potential to be used in moisture-resistant package materials.

3.3. *Mechanical properties*

Fig. 7 shows the mechanical properties of the coated films and dKGM. The tensile strength (σ_b) and elongation at break (ε_b) of dKGM was 36.2 MPa and 9.0%, respectively (Fig. 7a). While, the coated films dKGM-SSA0 which only contained shellac in the coating layer was 31.0 MPa, 1295 MPa and 13.3%, respectively (Fig. 7a and b), indicating that the shellac in the coating layer contributed to the enhancement of ε_b, but failed to enhance the σ_b and E of the coated films. However, the σ_b and E values increased simultaneously with the increase of the stearic acid content and reached maximum values of 41.0 MPa and 2069 MPa, respectively, for dKGM-SSA20 (Fig. 7a and b). It was mainly attributed to the uniform mixing between shellac and stearic acid in the coating layer. This also further confirmed that the shellac had intimate adhesion on the surface of dKGM, allowing coating layer to play a role in enhancement of mechanical properties. However, other study reported that the lipid layer such as acetem could increase the elongation for whey protein isolate film but had a negligible mechanical strength (Anker et al., 2002), which further confirmed the interaction effect of shellac and stearic acid on the enhancement of mechanical properties in our work.

4. Conclusions

The moisture-resistant konjac glucomannan films were successfully prepared by coating shellac/stearic acid with about 10 μm thickness to deacetylated konjac glucomannan films. When stearic acid content in the coating layer increased 5 up to 40 wt%, the moisture barrier properties and mechanical properties of the coated films were much improved compared with those of the dKGM and dKGM-SSA0 films. It was noteworthy that the coated film with 20 wt% stearic acid in the coating possessed the highest tensile strength of 41.0 MPa and modulus (2069 MPa). Shellac in the coating layer contributed to improving the optical transmittance of the coated films. Stearic acid in the coating played an important role in enhancing moisture barrier properties and mechanical properties of the coated films. The key factors for the enhancement of all the properties of the coated films should be attributed to the intimate interfacial adhesion between the coating layer and dKGM substrate, and the uniform mixing between shellac and stearic acid in the coating layer.

Acknowledgements

This work was supported by the Natural Science Foundation of Shandong Province (2012ZRC21003) and National Natural Science Foundation of China (31271837).

Appendix A.

See Figs. A.1 and A.2.

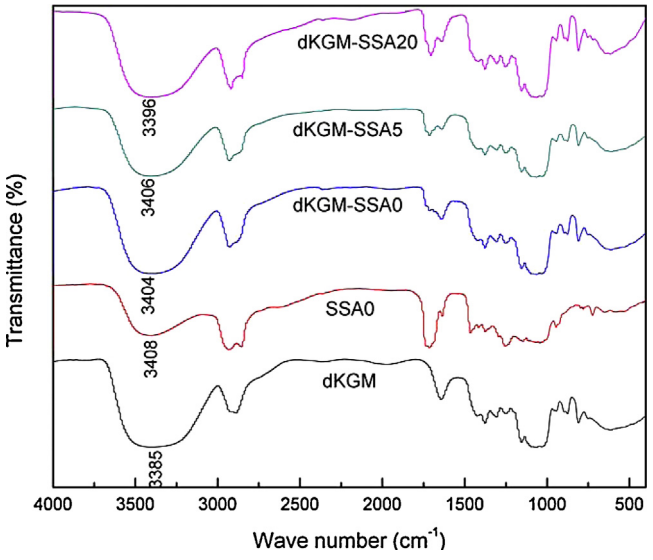

Fig. A.1. FTIR spectra of the dKGM film, shellac (SSA0), and the coated films.

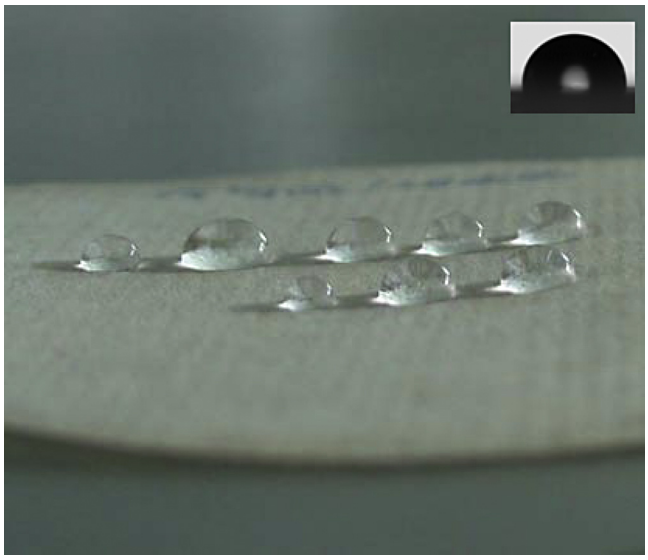

Fig. A.2. The photograph of the hydrophobic filter paper treated with shellac/stearic acid coating. Insets are the water contact angle.

References

Anker, M., Berntsen, J., Hermansson, A.-M., & Stading, M. (2002). Improved water vapor barrier of whey protein films by addition of an acetylated monoglyceride. *Innovative Food Science & Emerging Technologies*, *3*(1), 81–92.

Byun, Y., Ward, A., & Whiteside, S. (2012). Formation and characterization of shellac-hydroxypropyl methylcellulose composite films. *Food Hydrocolloids*, *27*(2), 364–370.

Cao, X., Deng, R., & Zhang, L. (2006). Structure and properties of cellulose films coated with polyurethane/benzyl starch semi-IPN coating. *Industrial & Engineering Chemistry Research*, *45*(12), 4193–4199.

Debeaufort, F., Quezada-Gallo, J.-A., Delporte, B., & Voilley, A. (2000). Lipid hydrophobicity and physical state effects on the properties of bilayer edible films. *Journal of Membrane Science*, *180*(1), 47–55.

Farag, Y., & Leopold, C. (2009). Physicochemical properties of various shellac types. *Dissolution Technologies*, *16*, 33–39.

He, M., Xu, M., & Zhang, L. (2013). Controllable stearic acid crystal induced high hydrophobicity on cellulose film surface. *ACS Applied Materials & Interfaces*, *5*(3), 585–591.

Jannerfeldt, G., Boogh, L., & Månson, J.-A. (2000). Tailored interfacial properties for immiscible polymers by hyperbranched polymers. *Polymer*, *41*(21), 7627–7634.

Jia, D., Fang, Y., & Yao, K. (2009). Water vapor barrier and mechanical properties of konjac glucomannan–chitosan–soy protein isolate edible films. *Food and Bioproducts Processing*, *87*(1), 7–10.

Jian, W., Zeng, Y., Xiong, H., & Pang, J. (2011). Molecular simulation of the complex of konjac glucomannan–borate in water. *Carbohydrate Polymers*, *85*(2), 452–456.

Jian, W. J., Wang, M., Yao, M. N., & Pang, J. (2010). Formation sites and microscopic conformation study on the Konjac Glucomannan molecular helices. *Chinese Journal of Structural Chemisty*, *29*, 1084–1090.

Li, J., Ji, J., Xia, J., & Li, B. (2012). Preparation of konjac glucomannan-based superabsorbent polymers by frontal polymerization. *Carbohydrate Polymers*, *87*(1), 757–763.

Limmatvapirat, S., Limmatvapirat, C., Luangtana-Anan, M., Nunthanid, J., Oguchi, T., Tozuka, Y., et al. (2004). Modification of physicochemical and mechanical properties of shellac by partial hydrolysis. *International Journal of Pharmaceutics*, *278*(1), 41–49.

Limmatvapirat, S., Limmatvapirat, C., Puttipipatkhachorn, S., Nuntanid, J., & Luangtana-Anan, M. (2007). Enhanced enteric properties and stability of shellac films through composite salts formation. *European Journal of Pharmaceutics and Biopharmaceutics*, *67*(3), 690–698.

Lu, Y., & Zhang, L. (2002). Interfacial structure and properties of regenerated cellulose films coated with superthin polyurethane/benzoyl konjac glucomannan coating. *Industrial & Engineering Chemistry Research*, *41*(5), 1234–1241.

Lu, Y., Zhang, L., & Xiao, P. (2004). Structure, properties and biodegradability of water resistant regenerated cellulose films coated with polyurethane/benzyl konjac glucomannan semi-IPN coating. *Polymer Degradation and Stability*, *86*(1), 51–57.

Luangtana-Anan, M., Limmatvapirat, S., Nunthanid, J., Wanawongthai, C., Chalongsuk, R., & Puttipipatkhachorn, S. (2007). Effect of salts and plasticizers on stability of shellac film. *Journal of Agricultural and Food Chemistry*, *55*(3), 687–692.

Luangtana-Anan, M., Nunthanid, J., & Limmatvapirat, S. (2010). Effect of molecular weight and concentration of polyethylene glycol on physicochemical properties and stability of shellac film. *Journal of Agricultural and Food Chemistry*, *58*(24), 12934–12940.

Maeda, M., Shimahara, H., & Sugiyama, N. (1980). Detailed examination of the branched structure of Konjac glucomannan. *Agricultural and Biological Chemistry*, *44*(2), 245–252.

Phan The, D., Debeaufort, F., Luu, D., & Voilley, A. (2008). Moisture barrier, wetting and mechanical properties of shellac/agar or shellac/cassava starch bilayer biomembrane for food applications. *Journal of Membrane Science*, *325*(1), 277–283.

Soradech, S., Limatvapirat, S., & Luangtana-Anan, M. (2013). Stability enhancement of shellac by formation of composite film: Effect of gelatin and plasticizers. *Journal of Food Engineering*, *116*(2), 572–580.

Soradech, S., Nunthanid, J., Limmatvapirat, S., & Luangtana-Anan, M. (2012). An approach for the enhancement of the mechanical properties and film coating efficiency of shellac by the formation of composite films based on shellac and gelatin. *Journal of Food Engineering*, *108*(1), 94–102.

Wang, J., Chen, L., & He, Y. (2008). Preparation of environmental friendly coatings based on natural shellac modified by diamine and its applications for copper protection. *Progress in Organic Coatings*, *62*(3), 307–312.

Wu, C., Peng, S., Wen, C., Wang, X., Fan, L., Deng, R., et al. (2012). Structural characterization and properties of konjac glucomannan/curdlan blend films. *Carbohydrate Polymers*, *89*(2), 497–503.

Wu, T., Pan, Y., & Li, L. (2010). Study on superhydrophobic hybrids fabricated from multiwalled carbon nanotubes and stearic acid. *Journal of Colloid and Interface Science*, *348*(1), 265–270.

Xie, Q., Fan, G., Zhao, N., Guo, X., Xu, J., Dong, J., et al. (2004). Facile creation of a bionic super-hydrophobic block copolymer surface. *Advanced Materials*, *16*(20), 1830–1833.

Xu, C., Luo, X., Lin, X., Zhuo, X., & Liang, L. (2009). Preparation and characterization of polylactide/thermoplastic konjac glucomannan blends. *Polymer*, *50*(15), 3698–3705.

Zhang, L., Xue, Q., Mo, Z., & Jin, X. (2006). *Modern Methods of Polymer Physics*. Wuhan: Wuhan University Press.